Polymer Chemistry

PAPER

View Article Online
View Journal

Cite this: DOI: 10.1039/c5py01900a

Synthesis of 9,9′-spirobifluorene-based conjugated microporous polymers by $FeCl_3$-mediated polymerization†

Arindam Modak, Yoshifumi Maegawa, Yasutomo Goto and Shinji Inagaki*

Received 30th November 2015,
Accepted 27th December 2015

DOI: 10.1039/c5py01900a

www.rsc.org/polymers

An easy, safe and low-cost synthesis of conjugated microporous polymers and related carbonized microporous materials is highly desirable for practical use. Here, we report the synthesis of 9,9′-spirobifluorene-based conjugated microporous organic polymers (COPs) starting from unsubstituted spirobifluorene using an inexpensive $FeCl_3$ mediator. Three kinds of COPs, synthesized by $FeCl_3$-mediated oxidative polymerization, Friedel–Crafts polymerization, and competitive oxidative/Friedel–Crafts polymerization of the spirobifluorene precursor, showed large surface areas (940–1980 $m^2\ g^{-1}$) and high micropore volumes (0.5–0.9 $cm^3\ g^{-1}$). The COPs synthesized by competitive oxidative/Friedel–Crafts polymerization were found to show a high gas uptake ability which is almost comparable to that of the previously reported spirobifluorene-based microporous organic polymers prepared by Yamamoto polymerization using an expensive Ni catalyst. The COPs were easily transformed into microporous carbons by direct carbonization without the addition of any activating agents. The carbonization process enhanced the gas uptake ability of the COPs at low pressure (1 atm), although the surface area and micropore volume were almost unchanged or slightly decreased. The $FeCl_3$-mediated competitive oxidative/Friedel–Crafts polymerization of non-functionalized aromatics would be a useful synthetic approach for an easy, safe and low-cost synthesis of conjugated microporous polymers.

Introduction

Conjugated microporous organic polymers (COPs) and related carbonized materials have attracted considerable attention as gas adsorbents and catalysts for environmental applications and energy production.[1–4] An easy, safe and low-cost synthesis of COPs is important for practical use. Recently, a versatile route to synthesize COPs that involves Friedel–Crafts polymerization of non-functionalized aromatic monomers in the presence of an inexpensive $FeCl_3$ mediator was reported. However, the aromatic monomers were limited to relatively simple aromatics such as benzene, substituted benzenes, biphenyl and 1,3,5-triphenylbenzene[5] and hydroxyl-containing fused aromatics such as naphthol and binaphthol.[6]

9,9′-Spirobifluorene, which features an sp^3-hybridized carbon with two perpendicularly aligned π systems, has been a compound of considerable interest for organic electronics.[7] Polymers synthesized from such a precursor could incorporate a 90° knot in each repeating unit, which efficiently restricts the packing of rigid polymer chains and creates a large, accessible free space. In addition, the three-dimensional topology of spirobifluorene is retained in polymeric structures. Conjugated microporous polymers based on a spirobifluorene moiety are expected to be more robust than polymers derived from a planar fluorene monomer.

Recently, Farha and Hupp group reported spirobifluorene-based conjugated microporous polymers and their thermal treatments to enhance gas-adsorption properties.[8] Although these results clearly demonstrate the utility of the spirobifluorene skeleton, the polymer network was developed by Yamamoto polymerization which requires brominated spirobifluorene and excess amounts of $Ni(cod)_2$ (cod: 1,5-cyclooctadiene) as a mediator. The synthesis and purification of such building blocks are quite complicated and consume much energy and time. The use of $Ni(cod)_2$ increases the synthetic costs and is dangerous due to its high flammability.

In this study, we focused on the synthesis of spirobifluorene-based conjugated microporous organic polymers starting from non-functionalized 9,9′-spirobifluorene in combination with a cheap $FeCl_3$ mediator. $FeCl_3$ is not only a strong Lewis acid for Friedel–Craft reactions but also a typical oxidant for oxidative coupling in the synthesis of polyaromatic hydrocar-

Toyota Central R&D Laboratories., Inc., Nagakute, Aichi 480-1192, Japan. E-mail: inagaki@mosk.tytlabs.co.jp

†Electronic supplementary information (ESI) available: Detail characterization of COPs and carbonized COPs and synthetic procedure of COP-3F and its nitrogen adsorption/desorption isotherms. See DOI: 10.1039/c5py01900a

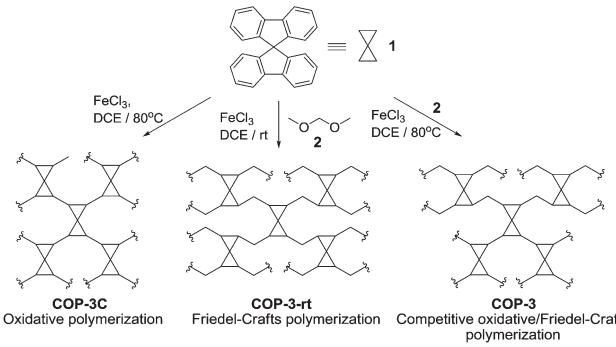

Scheme 1 Synthesis of spirobifluorene-based conjugated organic polymers **COP-3C**, **COP-3-rt**, and **COP-3** by $FeCl_3$-mediated polymerization.

bons and semiconducting polymers such as polythiophene.[5,9] Based on these findings, we synthesized three types of spirobifluorene-based COPs by iron-mediated polymerization approaches considering (1) oxidative polymerization, (2) Friedel–Crafts polymerization, and (3) competitive oxidative/Friedel–Crafts polymerization (Scheme 1). The resulting microporous polymers were further carbonized to give microporous carbons. The gas adsorption properties of the COPs and carbonized COPs at low pressure (<1 atm) were investigated.

Experimental

Materials

9,9′-Spirobifluorene and dry 1,2-dichloroethane (DCE) were obtained from Sigma-Aldrich. Dimethoxymethane was purchased from Tokyo Chemical Industry Co., Ltd. Anhydrous $FeCl_3$, dimethoxymethane, and other reagents, including all solvents, were obtained from Wako Pure Chemical Industries, Ltd, and used without purification.

Characterization

X-ray diffraction (XRD) of samples was performed using a RINT-TTR diffractometer (Rigaku) with Cu-Kα radiation (50 kV, 300 mA). Scanning electron microscopy (SEM) images were obtained on an SU3500 (Hitachi) instrument at an acceleration voltage of 5–10 kV. ^{13}C cross-polarization (CP) MAS NMR measurements were performed at 100 MHz at a sample spinning frequency of 5 kHz using an Avance 400 spectrometer (Bruker) with a 7 mm zirconia rotor. The repetition delay was 5 s, the contact time was 1.75 ms, and the pulse width was 4.5 μs (^1H 90° pulse). Fourier transform infrared (FT-IR) spectra were recorded using a Nicolet Avatar-360 FT-IR spectrometer (Thermo Fisher Scientific) with an attenuated total reflection (ATR) attachment. UV/vis absorption spectra were recorded using a V-670 spectrometer (JASCO), and the samples were diluted to 0.1 wt% using $BaSO_4$. Thermogravimetric (TG) analysis was carried out by using a Thermo plus TG8120 (Rigaku) instrument under flowing air (0.5 L min^{-1}). The rate of temperature increase was 10 °C min^{-1}. X-ray photoelectron spectroscopy (XPS) was performed with an ULVAC Quantera SXM using Al Kα as the X-ray source. The amount of residual iron in the samples was measured using an inductively coupled plasma (ICP) spectrometer, CIROS 120EOP (Rigaku), with 259.9 nm as the wavelength for Fe determination. Raman spectra were obtained using an NRS-3300 Raman spectrometer (JASCO). Gas sorption isotherms were measured using an Autosorb-1 (Quantachrome) instrument. The purities of the gases were as follows: N_2, >99.999%, CO_2, >99.995%, CH_4, >99.999%, and H_2, >99.99%. The Brunauer–Emmett–Teller (BET) surface areas of the samples were calculated from nitrogen adsorption isotherms over a pressure range from 0.01 to 0.1 P/P_0. Micropore volumes were evaluated from the intercept of the *t*-plot (Fig. S8†). Characteristic adsorption energies (E_0) were obtained from the slope of Dubinin–Radushkevich (DR) plots using an affinity coefficient (β) of 0.33 (Fig. S9†).[10] The average pore sizes (w_{ave}) were calculated based on the equation proposed by Dubinin, $w_{ave} = K/E_0$, where K is an empirical constant.[11] The same K value with a series of activated carbons (17.5 nm kJ mol^{-1})[11] was used for the calculation against the carbonized COPs.

Synthesis of COP-3

A 30 mL two-neck flask connected to a condenser was charged with a stirring bar, 9,9′-spirobifluorene (**1**, 400 mg, 1.26 mmol), and anhydrous $FeCl_3$ (817 mg, 5.0 mmol). The flask was thoroughly evacuated and filled with argon. Dry 1,2-dichloroethane (5 mL) was then added, and the mixture was stirred for 5 min. During stirring, the color of the reaction mixture turned purple-red. Next, dimethoxymethane (**2**, 453 mg, 5.9 mmol) was added slowly through a syringe with continuous stirring. During the addition of **2**, the color faded from deep purple-red to dirty yellow. The reaction mixture was stirred for 15 min at room temperature and refluxed at 80 °C for 24 h. After the reaction, the resulting dirty solid was filtered and thoroughly washed with water, tetrahydrofuran, methanol and 6 N aq. HCl. Washing was continued until the filtrate became colorless. The resulting material was extracted with methanol for 24 h by Soxhlet extraction. The resulting powder was dried under reduced pressure at 60 °C to give **COP-3** (260 mg, 65% yield) as a yellow-orange powder. The residual amount of Fe was <50 ppm. IR (ATR): ν_{max} 2900, 1441, 1282, 1147, 1007 cm^{-1}; ^{13}C CP MAS NMR (100 MHz): δ 151.3, 141.5, 134.1, 129.1, 125.0, 121.2, 75.0, 67.6, 54.9, 42.0, 21.2. Elemental analysis: C (85.55), H (4.66), Cl (4.46), O (4.05) (the amount O in the polymer was estimated by XPS data).

Synthesis of COP-3-rt

In a typical synthesis approach, a 30 mL two-neck flask connected to a condenser was charged with a stirring bar, **1** (400 mg, 1.26 mmol), and anhydrous $FeCl_3$ (817 mg, 5.0 mmol). The flask was thoroughly evacuated and filled with argon. Dry 1,2-dichloroethane (5–6 mL) was then added, and the mixture was stirred for 5 min. During stirring, the color of the reaction mixture turned purple-red. Next, **2** (453 mg,

5.9 mmol) was added slowly through a syringe with continuous stirring. During the addition of **2**, the color faded from deep purple-red to dirty yellow. The reaction mixture was stirred for 3 more days at room temperature (25 °C). The filtered sample was washed using exactly the same procedure as for **COP-3**. The resulting powder was dried under reduced pressure at 60 °C to give **COP-3-rt** (252 mg, 63% yield) as a pale yellow powder. The residual amount of Fe was 250 ppm. IR (ATR): ν_{max} 2990, 1400, 1280, 1150 cm^{-1}; ^{13}C CP MAS NMR (100 MHz): δ 151.6, 141.6, 133.9, 129.0, 125.1, 121.7, 75.0, 67.1, 54.9, 42.0, 21.2. Elemental analysis: C (84.29), H (4.47), Cl (2.73), O (5.35) (the amount O in the polymer was estimated by XPS data).

Synthesis of COP-3C

A 30 mL two-neck flask connected to a condenser was charged with a stirring bar, **1** (400 mg, 1.26 mmol), and anhydrous $FeCl_3$ (817 mg, 5.0 mmol). The flask was thoroughly evacuated and filled with argon. Dry 1,2-dichloroethane (5–6 mL) was added and the mixture was stirred for 5 min. The mixture was then refluxed at 80 °C for 24 h. After the reaction, the sample was filtered and washed using the same procedure for **COP-3**. The resulting powder was dried under reduced pressure at 60 °C to give **COP-3C** (240 mg, 60% yield) as an orange-yellow powder. The residual amount of Fe was 130 ppm. IR (ATR): ν_{max} 2900, 1405, 1270, 1125 cm^{-1}; ^{13}C CP MAS NMR (100 MHz): δ 150.8, 142.7, 128.8, 124.9, 121.5, 67.9. Elemental analysis: C (88.27), H (4.17), Cl (4.30).

Carbonization of COPs

Carbonization was carried out for all COPs without the addition of activating agents or templates. The samples, in an alumina crucible, were placed in a quartz tube furnace at a heating rate of 10 °C min^{-1} under a continuous flow of N_2 (100 mL min^{-1}) and maintained at 600 °C for 6 h. The resulting black powders were named **COP-3-600**, **COP-3-rt-600**, and **COP-3C-600**, respectively. The char yields of **COP-3-600**, **COP-3-rt-600**, and **COP-3C-600** based on weight loss during the carbonization were 65%, 72% and 90%, respectively.

Results and discussion

Synthesis and characterization of COPs

Three types of spirobifluorene-based conjugated organic polymers were synthesized by $FeCl_3$-mediated polymerization of 9,9′-spirobifluorene (**1**), as shown in Scheme 1. We carefully investigated the polymerization behaviors for oxidative polymerization of **1**, Friedel–Crafts polymerization of **1** and dimethoxymethane **2**, and competitive oxidative/Friedel–Crafts polymerization of **1** and **2**. The conjugated organic polymers were characterized by elemental analysis, XPS and ICP measurements, ^{13}C CP MAS NMR (Fig. 1), nitrogen adsorption/desorption isotherms (Fig. 2), UV/vis diffuse reflectance spectroscopy (Fig. 3), FT-IR (Fig. S1†), XRD (Fig. S2†), TG (Fig. S3–4†), and SEM (Fig. S5†).

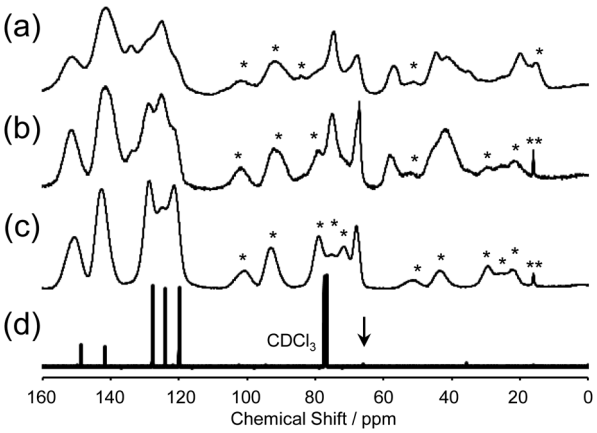

Fig. 1 ^{13}C CP MAS NMR spectra of **COP-3** (a), **COP-3-rt** (b), and **COP-3C** (c), and ^{13}C NMR spectrum of **1** in $CDCl_3$ (d); *spinning side bands.

Oxidative polymerization of **1** efficiently proceeded at 80 °C in 1,2-dichloroethane to give a non-soluble orange-yellow powder (**COP-3C**) in 60% yield based on **1**. However, the reaction was very sluggish under milder oxidative polymerization conditions (at 25 °C) and did not produce a non-soluble polymer. This was probably due to the lower reactivity of the fluorene rings owing to the bulky spiro structure of **1**. Thus, the carbon–carbon bond formation between units of **1** requires heating conditions to form the conjugate structure of **COP-3C**. To evaluate the chemical structure of **COP-3C**, the ^{13}C CP MAS NMR spectrum was recorded (Fig. 1). The chemical shifts of **COP-3C** were similar to those of **1** in $CDCl_3$, and there were no detectable peaks assignable to the byproducts or fragments of **1**. However, elemental analysis indicated the presence of a small amount of chlorine. Although this implies that chlorination partially occurs under this condition, a polymer network of **COP-3C** would be mainly produced by the oxidative homo-coupling of **1**. The ICP measurement showed that the residual Fe amount was 130 ppm in the **COP-3C**.

Friedel–Crafts polymerization of **1** and **2** was carried out in 1,2-dichloroethane at room temperature (~25 °C) to minimize competitive oxidative coupling of **1**. The reaction proceeded even at room temperature to afford a non-soluble polymer (**COP-3-rt**) in 63% yield; the reaction time required was 3 days. The color of **COP-3-rt** was pale yellow, suggesting that the π-conjugation length of **COP-3-rt** was shorter than that of **COP-3C**. This observation indicates the successful suppression of oxidative coupling of **1** under the Friedel–Crafts polymerization conditions. We also found that no polymerized product was obtained under these reaction conditions in the absence of **2**. These results suggest that **2** acts as a cross-linking reagent for **COP-3-rt**. The incorporation of cross-linkage was directly confirmed by ^{13}C CP MAS NMR measurement. The ^{13}C CP MAS NMR spectrum showed several aliphatic peaks which may have been due to the Friedel–Crafts reaction between **1** and **2**. The aliphatic peaks were assignable to a methylene

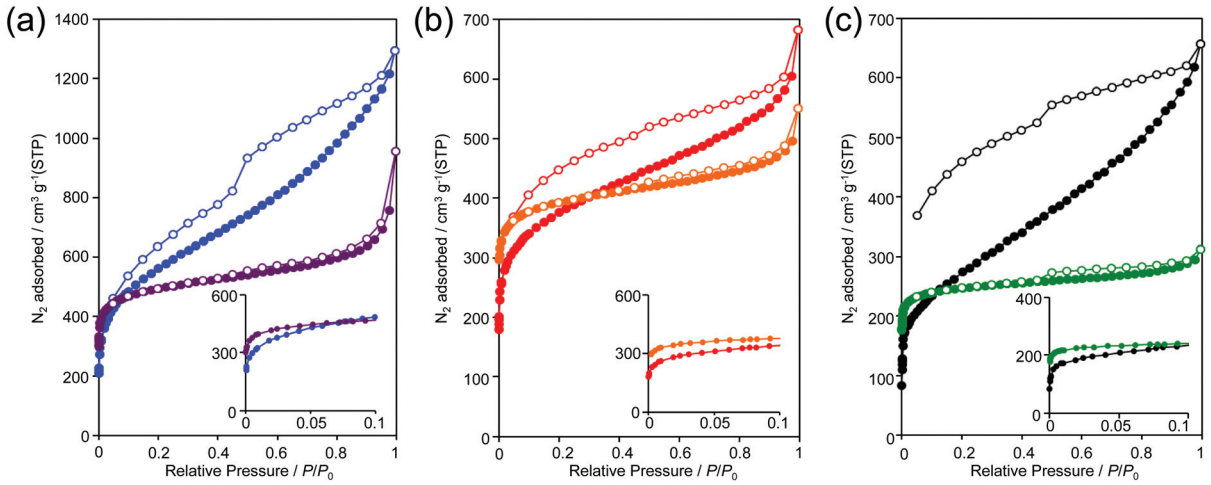

Fig. 2 Nitrogen adsorption/desorption isotherms of COPs and carbonized COPs. (a) **COP-3** (blue) and **COP-3-600** (purple); (b) **COP-3-rt** (red) and **COP-3-rt-600** (orange); and (c) **COP-3C** (black) and **COP-3C-600** (green). Inset: nitrogen adsorption isotherms at low relative pressure (0–0.1).

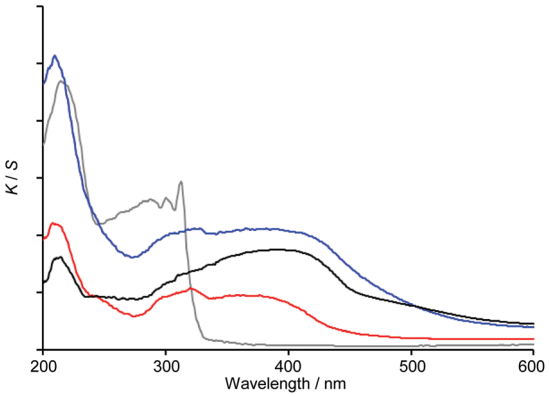

Fig. 3 UV/vis diffuse reflectance spectra of **COP-3** (blue line), **COP-3-rt** (red line), **COP-3C** (black line), and **1** (gray line).

carbon (42 ppm), a benzyl carbon (75 ppm), and a methoxy carbon (54.9 ppm). These peaks are commonly observed in Friedel–Crafts polymerization of thiophene or pyrrole and **2**.[12] The presence of an oxygen atom was confirmed by XPS measurement. This supports the view that methoxylation also occurs between **1** and **2** in the presence of $FeCl_3$. The ^{13}C CP MAS NMR spectrum showed that the aromatic peaks attributed to the fluorene rings in **COP-3-rt** were slightly broadened and shifted compared with those of **COP-3C**. These changes also suggest substitution of the spirobifluorene skeleton with methylene groups or aliphatic fragments. The residual Fe amount in **COP-3-rt** was 250 ppm, which was higher than that of **COP-3C**.

Competitive oxidative/Friedel–Crafts polymerization of **1** and **2** was conducted in 1,2-dichloroethane under heating conditions at 80 °C. The reaction generated a non-soluble polymer (**COP-3**) within 24 h in 65% yield. The color of **COP-3** was yellow-orange, which was similar to that of **COP-3C**. This implies an extension of the π-conjugation length of **COP-3** compared with that of **COP-3-rt**. This observation explains why the increased reaction temperature enhanced the reaction efficiency of oxidative coupling as well as the Friedel–Crafts reaction. Thus, the polymer chain of **COP-3** is likely to be constructed through competitive polymerization between oxidative coupling and the Friedel–Crafts reaction. The ^{13}C CP MAS NMR spectrum of **COP-3** showed broad aromatic peaks and several aliphatic peaks. The elemental analysis revealed the presence of chlorine and oxygen atoms in the polymer. These results also suggest sufficient oxidative coupling and Friedel–Crafts reaction. A detailed investigation of the chemical structures of these polymers is currently underway in our laboratory. The ICP measurement showed <50 ppm of the Fe atom in the **COP-3**, which was lower than those of **COP-3C** and **COP-3-rt**.

Nitrogen adsorption/desorption isotherms were measured to investigate the porosity of **COP-3**, **COP-3-rt**, and **COP-3C** (Fig. 2). The isotherms exhibited a steep increase at lower P/P_0 values (under 0.05) due to microporosity, and a gradual increase in adsorption at higher P/P_0 values due to broad mesoporosity. Analysis of the isotherms revealed that the polymers had highly porous structures with large BET surface areas (940–1980 $m^2\ g^{-1}$) and high micropore volumes (0.5–0.9 $cm^3\ g^{-1}$) (Table 1). The pore size distributions of COPs were obtained by QSDFT analysis of the adsorption isotherms, which showed that COPs contain micropores of around 1 nm (Fig. S10†). The reason for the highly porous structures was attributed to the unique polymer networks containing bulky spirobifluorene units. Indeed, the polymer synthesized by oxidative polymerization of the non-bulky 9,9′-dimethylfluorene (**COP-3F**) exhibited very small porosity, with a surface area of 70 $m^2\ g^{-1}$ (Fig. S6†). This result supports the contention that the introduction of perpendicularly aligned fluorene units in the polymer contributes to the highly porous structure of COPs. The isotherms show large hysteresis *i.e.*, the desorption branches of the isotherms of COPs are not close to the adsorption branches even at low relative pressure. This is sometimes observed for porous polymer networks, suggesting pressure-

Table 1 Surface areas, pore volumes, and gas uptake properties of the samples

Samples	S_{BET} (m^2 g^{-1})	V_{micro} (cm^3 g^{-1})	CO_2 uptake at 273 K (mmol g^{-1})	CH_4 uptake at 273 K (mmol g^{-1})	H_2 uptake at 77 K (wt%)
COP-3	1980	0.9	4.6	1.4	1.9
COP-3-rt	1490	0.6	3.5	0.9	1.4
COP-3C	940	0.5	2.1	0.7	1.1
COP-3-600	1860	0.7	5.2	1.9	2.2
COP-3-rt-600	1370	0.6	5.4	2.0	2.1
COP-3C-600	950	0.4	4.3	1.6	1.8

dependent structural changes. This behavior is mostly attributed to the swelling of the polymer matrix, demonstrating the softness of the framework.[13]

UV/vis diffuse reflectance measurements were carried out to examine the optical properties of **COP-3**, **COP-3-rt**, and **COP-3C** (Fig. 3). All polymers showed broad absorption bands in the visible region, which were quite different from those of the precursor **1**. The visible absorption bands indicated the presence of an extended π-conjugated structure in these polymers. **COP-3** and **COP-3C**, in particular, showed strong visible light absorption bands with an edge at 550 nm. This can be explained on the basis of sufficient oxidative coupling of spirobifluorene units under heating conditions. In contrast, **COP-3-rt** exhibited weak visible light absorption abilities, possibly due to the low degree of oxidative coupling of spirobifluorene units and the incorporation of methylene linkers in the polymer chain structure.

Thermogravimetric analyses were carried out to test the thermal stability of COPs. Under a nitrogen atmosphere, **COP-3C** showed almost no weight loss up to 500 °C, possibly due to the strong aromatic carbon–carbon covalent bonding network. By comparison, **COP-3** and **COP-3-rt** displayed approximately 6 wt% weight losses at 300–500 °C, attributable to aliphatic hydrocarbons attached on the spirobifluorene skeleton. In air, all COPs showed significant weight losses over 350 °C (Fig. S3†).

Carbonization of COPs

Three COPs were subjected to carbonization without the use of an activating agent. Carbonization was conducted at 600 °C for 6 h under a continuous flow of nitrogen. TG analysis under carbonization condition showed that the char yields of **COP-3C**, **COP-3-rt**, and **COP-3** were 90%, 72%, and 65%, respectively. This means 10–35% weight losses during the carbonization (Fig. S4†). XRD patterns of the carbonized COPs showed broad peaks around at 2θ = 23°, which is probably based on an interlayer structure of graphitic carbon (Fig. S2†). However, the peaks were very broad, suggesting an amorphous structure. In the FT-IR spectra, most of peaks from 800 to 2000 cm^{-1} and around 3000 cm^{-1} disappeared after carbonization (Fig. S1†). The elemental analyses of carbonized COPs indicated an increase of the carbon/hydrogen ratio. These results mean that there was almost complete decomposition of the organic groups and H_2 elimination from the framework of the COPs due to carbonization. Raman spectra were also recorded to elucidate the local structure of the carbonized COPs (Fig. S7†). D bands at 1350 cm^{-1} and G bands at 1600 cm^{-1} were observed for all samples. The broad peaks suggested that the frameworks had a disordered graphitic carbon structure, which was consistent with XRD results. TG analysis indicated that the carbonized COPs were stable up to 450 °C in air (~5% mass lost, Fig. S3†).

The shapes of the nitrogen adsorption/desorption isotherms of the carbonized COPs were different from those of the COPs before carbonization (Fig. 2). The isotherms showed a steep increase at low P/P_0 but a small increase at medium P/P_0, indicating typical microporous materials with almost no mesoporosity. The BET surface areas, micropore volumes and pore distribution were almost the same as those of the COPs before carbonization (Table 1, Fig. S10†). These results clearly indicate that the highly microporous structure was completely preserved even after thermal treatment, although direct carbonization without any activating agent usually results in a collapse of the porous structure of the original polymer.[14,15] This was probably due to the stable framework, with bulky spirobifluorene groups embedded in the structure.[8] We also observed that the amount of nitrogen adsorbed at very low P/P_0 (below 0.01) increased after carbonization (Fig. 2, inset). This suggested that the micropores became smaller after carbonization due to shrinkage of the COP frameworks during carbonization. We calculated the pore sizes of the carbonized COPs using a DR plot, assuming that they had the same surface properties as activated carbons (Fig. S9†). The calculated pore diameters were 0.78, 0.78, and 0.60 nm for **COP-3-600**, **COP-3-rt-600**, and **COP-3C-600**, respectively. Interestingly, **COP-3C-600** had a smaller pore size compared to **COP-3-600** and **COP-3-rt-600**. This was thought to be related to the non-existence of a methylene linker in the framework of **COP-3C**, which results in greater shrinkage of the framework structure compared to **COP-3** and **COP-3-rt** with methylene linkers. The large hysteresis loop observed in the adsorption/desorption isotherms for **COP-3** almost disappeared after carbonization, suggesting that the softness of the COP framework was lost in the carbonization process.

Gas uptake ability of COPs and carbonized COPs

We measured the adsorption–desorption isotherms of carbon dioxide (CO_2), methane (CH_4) at 273 K and hydrogen (H_2) at

77 K for COPs and carbonized COPs at low pressure (<1 atm) (Fig. S11, S12, and S13†). The gas uptakes at 1 atm are listed in Table 1. The gas uptakes decreased in the order **COP-3** < **COP-3-rt** < **COP-3C**, because the surface areas and micropore volumes decreased in this order. Interestingly, the gas uptakes increased dramatically after carbonization, by a factor of 1.1–2.3, although the surface areas and pore volumes were almost constant or decreased slightly during carbonization (Table 1). The improvement in gas uptake was attributed to changes in the pore surface properties and narrowing of the micropores during carbonization. Recent studies have revealed that a pore size of less than 1 nm is preferable in order to achieve adsorption of gases with a similar molecular size, such as CO_2 and CH_4, at ambient temperature.[16,17]

COP-3-600 and **COP-3-rt-600** showed high gas uptake ability in the low pressure region (< 1 atm), which was comparable with other porous carbons, polymers and MOFs with the highest gas adsorption abilities. For example, the CO_2 uptake (5.4 mmol g^{-1}, 273 K, 1 atm) for **COP-3-rt-600** was comparable with those of other porous polymers (3–6 mmol g^{-1}, 273 K, 1 atm),[18] MOFs (2.7–4.8 mmol g^{-1}, 273 K, 1 atm),[19] and activated carbon (3.5 mmol g^{-1}, 277 K, 120 kPa).[20] The CH_4 uptake ability of **COP-3-rt-600** (2 mmol g^{-1}, 273 K) was comparable with other adsorbents such as porous carbons (1.5–1.8 mmol g^{-1}, 298 K)[21] and MOFs such as NU-135 (1 mmol g^{-1}, 298 K).[22] However, the H_2 uptake at 77 K by **COP-3-600** (2.2 wt%) was found to be lower than that of activated carbon (2.8 wt%, 1 bar),[23] but comparable with those of poly(vinylidene chloride)-based carbon (2.5 wt%,)[24] and MOF-74s (1.8–2.5 wt%).[25] In addition, the reusability of the samples for CO_2 adsorption was confirmed by recycling experiments (Fig. S14†).

Conclusions

Spirobifluorene-based conjugated microporous polymers (COPs) were easily synthesized from non-functionalized 9,9′-spirobifluorene using an inexpensive $FeCl_3$ mediator. The π-conjugated spirobifluorene networks were mainly constructed by oxidative coupling and featured a strong visible-light-absorbing framework. Cross-linked spirobifluorene networks with methylene linkages were obtained by Friedel–Crafts reaction with dimethoxymethane, forming a flexible framework with less visible light absorption ability. The COPs were easily transformed into carbonized COPs by direct carbonization without the addition of any activating agent. The carbonized COPs showed high gas uptake ability, comparable with those of conventional porous carbons, porous polymers, and MOF-based adsorbents at low pressure.

Acknowledgements

This work was supported by ACT-C, JST. This work was supported in part by a Grant-in-Aid for Scientific Research on Innovative Areas ‘Artificial Photosynthesis’ (no. 2406) from the Japan Society for the Promotion of Science (JSPS). The authors acknowledge Dr Norihiko Setoyama (Toyota Central R&D Laboratories, Inc.) for helpful discussion against the gas sorption analysis. The authors also thank Mr Satoru Kosaka (Toyota Central R&D Laboratories, Inc.) for ICP analysis.

References

1 (*a*) O. K. Farha, A. M. Spokoyny, B. G. Hauser, Y. S. Bae, S. E. Brown, R. Q. Snurr, C. A. Mirkin and J. T. Hupp, *Chem. Mater.*, 2009, **21**, 3033; (*b*) Z. Xiang, D. Cao and L. Dai, *Polym. Chem.*, 2015, **6**, 1896.
2 (*a*) C. Xu and N. Hedin, *J. Mater. Chem. A*, 2013, **1**, 3406; (*b*) C. Pei, T. Ben and S. Qiu, *Mater. Horiz.*, 2015, **2**, 11.
3 (*a*) L. Chen, Y. Honsho, S. Seki and D. Jiang, *J. Am. Chem. Soc.*, 2010, **132**, 6742; (*b*) J. X. Jiang, A. Trewin, D. J. Adams and A. I. Cooper, *Chem. Sci.*, 2011, **2**, 1777.
4 (*a*) P. Serp, M. Corrias and P. Kalck, *Appl. Catal., A*, 2003, **253**, 337; (*b*) S. Li, G. Li, G. Li and G. Wu, *Microporous Mesoporous Mater.*, 2011, **143**, 22; (*c*) F. H. Richter, Y. Meng, T. Klasen, L. Sahraoui and F. Schüth, *J. Catal.*, 2013, **308**, 341.
5 B. Li, R. Gong, W. Wang, X. Huang, W. Zhang, H. Li, C. Hu and B. Tan, *Macromolecules*, 2011, **44**, 2410.
6 R. Dawson, L. A. Stevens, T. C. Drage, C. E. Snape, M. W. Smith, D. J. Adams and A. I. Cooper, *J. Am. Chem. Soc.*, 2012, **134**, 10741.
7 T. P. I. Saragi, T. Spehr, A. Siebert, T. F. Lieker and J. Salbeck, *Chem. Rev.*, 2007, **107**, 1011.
8 B. G. Hauser, O. K. Farha, J. Exley and J. T. Hupp, *Chem. Mater.*, 2013, **25**, 12.
9 A. A. O. Sarhanw and C. Bolm, *Chem. Soc. Rev.*, 2009, **38**, 2730.
10 L. Castelló, D. Cazorla-Amorós and A. Linares-Solano, *Carbon*, 2004, **42**, 1231.
11 F. Rouquerol, J. Rouquerol and K. Sing, *Adsorption by Powders and Porous Solids*, Academic Press, San Diego, 1999, p 225.
12 Y. Luo, B. Li, W. Wang, K. Wu and B. Tan, *Adv. Mater.*, 2012, **24**, 5703.
13 J. Weber, M. Antonietti and A. Thomas, *Macromolecules*, 2008, **41**, 2880.
14 M. Hu, J. Reboul, S. Furukawa, N. J. Torad, Q. Ji, P. Srinivasu, K. Ariga, S. Kitagawa and Y. Yamauchi, *J. Am. Chem. Soc.*, 2012, **134**, 2864.
15 T. Ben, Y. Li, L. Zhu, D. Zhang, D. Cao, Z. Xiang, X. Yao and S. Qiu, *Energy Environ. Sci.*, 2012, **5**, 8370.
16 Y. Li, T. Ben, B. Zhang, Y. Fu and S. Qiu, *Sci. Rep.*, 2013, **3**, 2420.
17 (*a*) V. Presser, J. McDonough, S. H. Yeon and Y. Gogotsi, *Energy Environ. Sci.*, 2011, **4**, 3059; (*b*) Z. Zhang, J. Zhou, W. Xing, Q. Xue, Z. Yan, S. Zhuo and S. Z. Qiao, *Phys. Chem. Chem. Phys.*, 2013, **15**, 2523.
18 C. Xu and N. Hedin, *Mater. Today*, 2014, **17**, 397.

19 Y. Liu, Z. U. Wang and H. C. Zhou, *Greenhouse Gases: Sci. Technol.*, 2012, **2**, 239.
20 A. Samanta, A. Zhao, G. K. H. Shimizu, P. Sarkar and R. Gupta, *Ind. Eng. Chem. Res.*, 2012, **51**, 1438.
21 J. Alcañiz-Monge, M. A. De La Casa-Lillo, D. Cazorla-Amorós and A. Linares-Solano, *Carbon*, 1997, **35**, 291.
22 R. D. Kennedy, V. Krungleviciute, D. J. Clingerman, J. E. Mondloch, Y. Peng, C. E. Wilmer, A. A. Sarjeant, R. Q. Snurr, J. T. Hupp, T. Yildirim, O. K. Farha and C. A. Mirkin, *Chem. Mater.*, 2013, **25**, 3539.
23 L. Zubizarreta, E. I. Gomez, A. Arenillas, C. O. Ania, J. B. Parra and J. J. Pis, *Adsorption*, 2008, **14**, 557.
24 J. Cai, J. Qi, C. Yang and X. Zhao, *ACS Appl. Mater. Interfaces*, 2014, **6**, 3703.
25 T. Pham, K. A. Forrest, R. Banerjee, G. Orcajo, J. Eckert and B. Space, *J. Phys. Chem. C*, 2015, **119**, 1078.